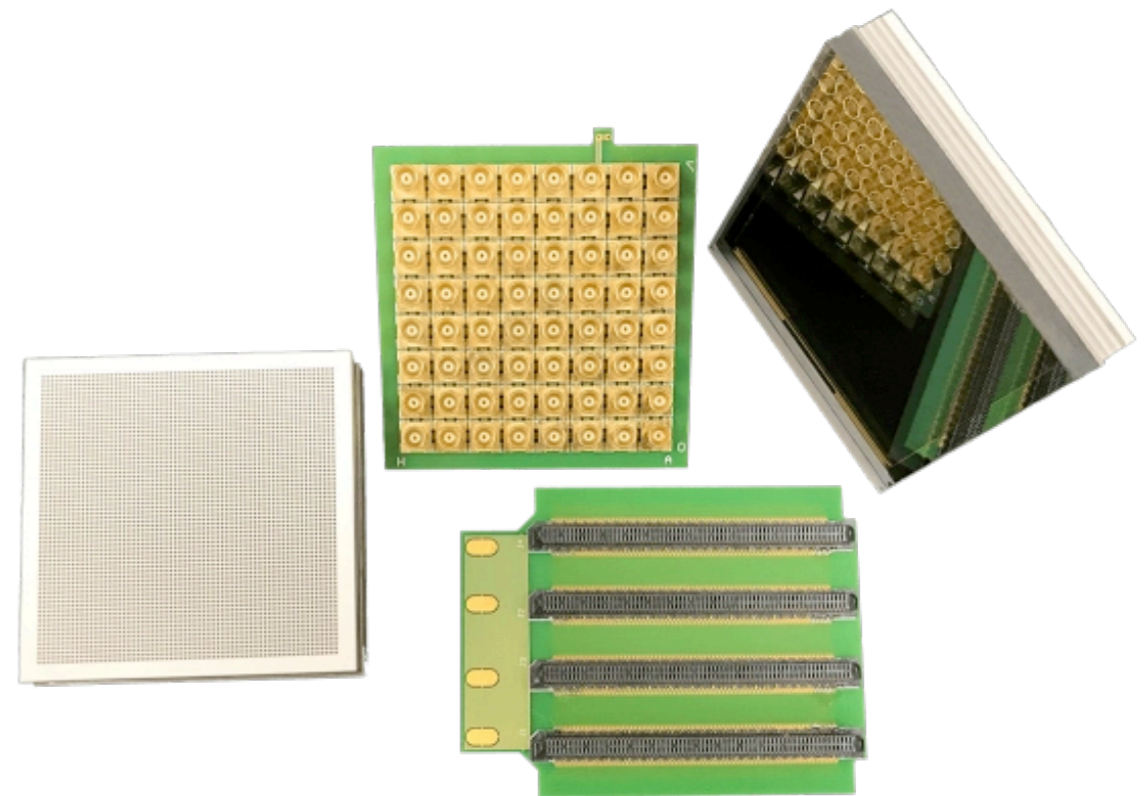
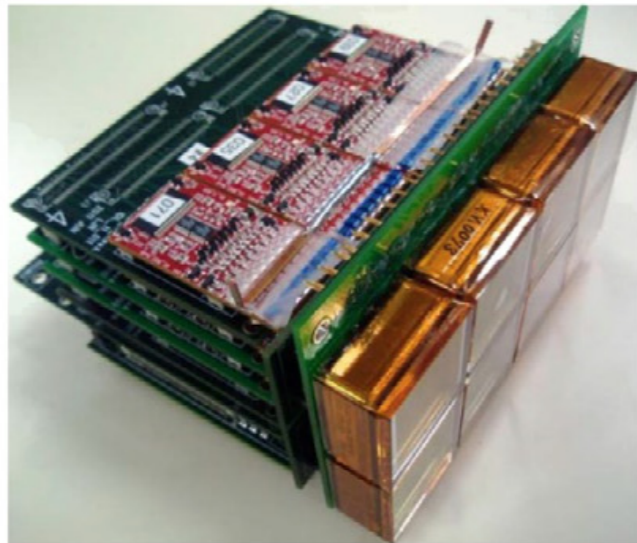
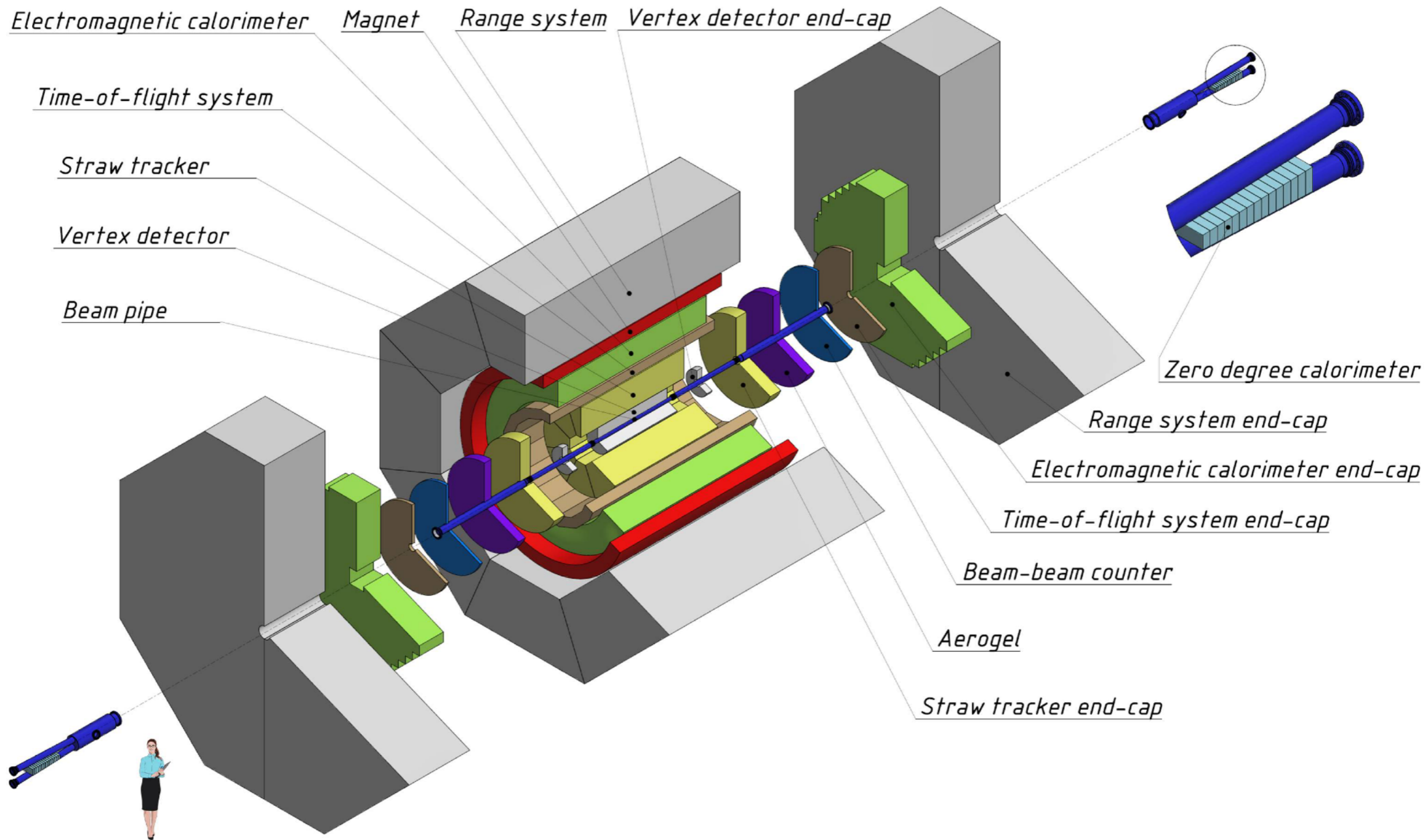


# Multi-anode MCP-PMT for ARICH detector of SPD

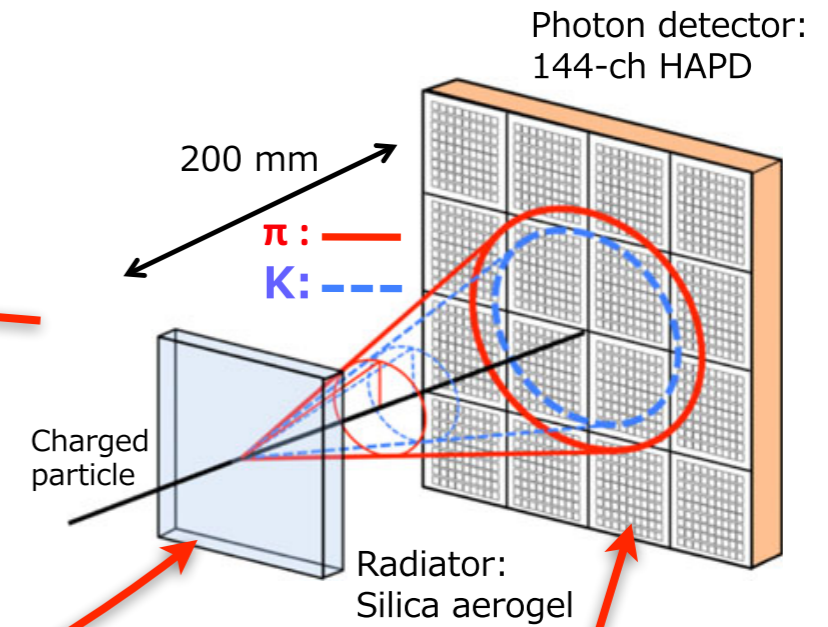
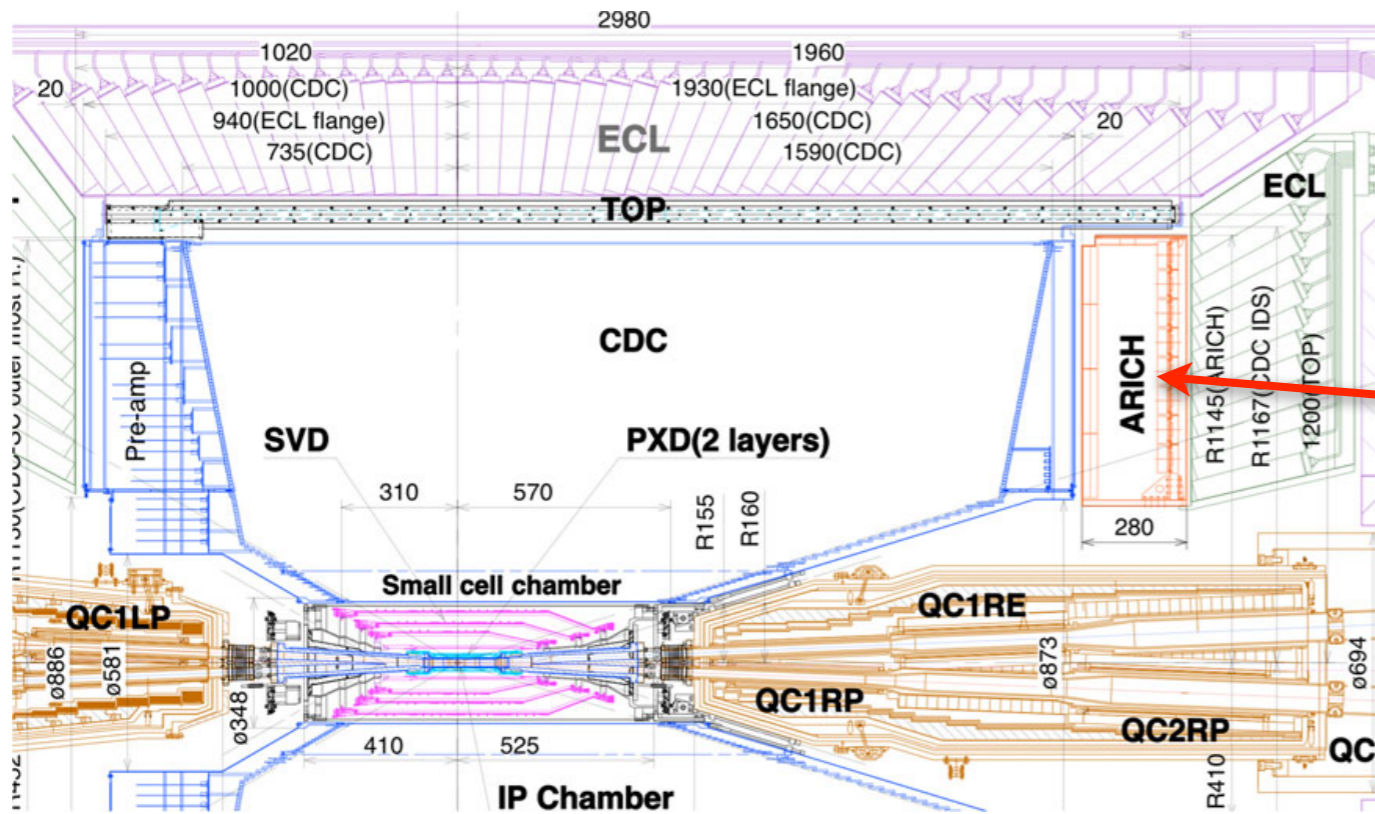
A.Korzenev, A.Kulikov



# SPD setup (TDR, Jan 2023)

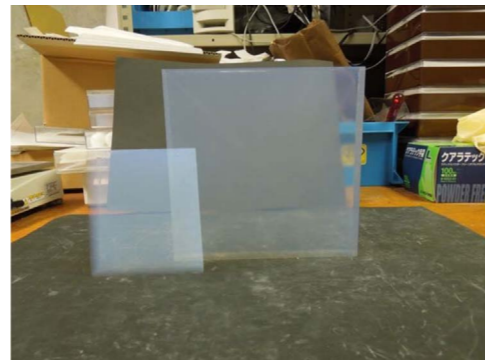
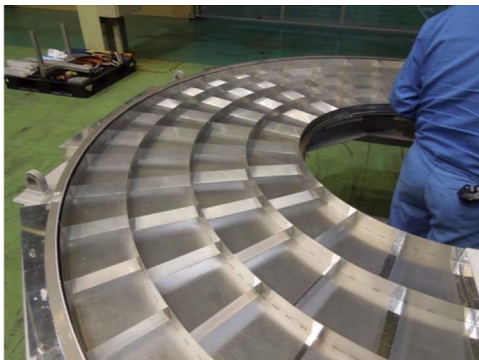
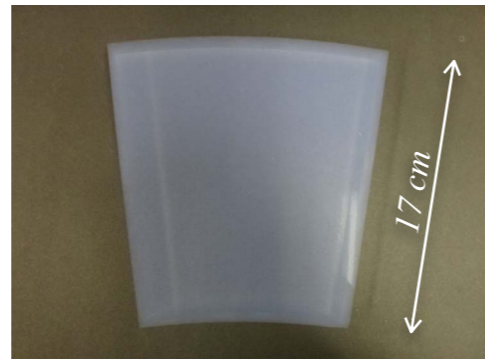


# ARICH (in endcap) of the Belle II experiment

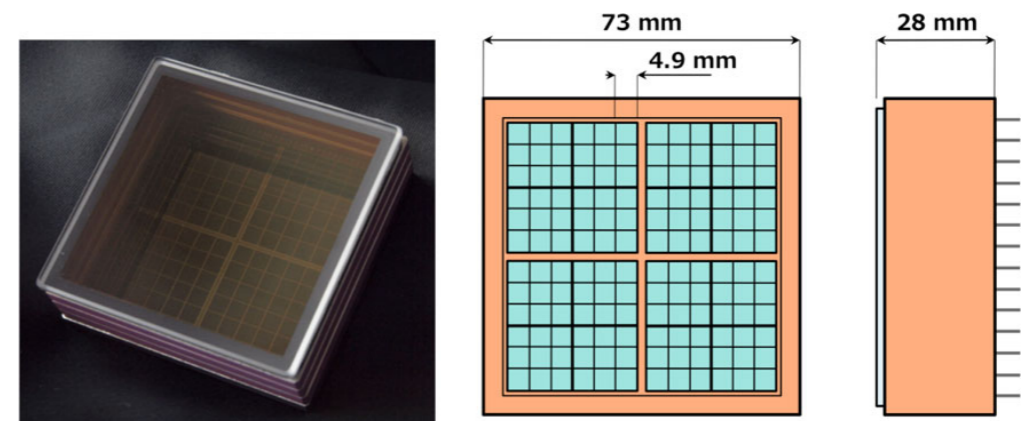


## Dual-Aerogel radiator

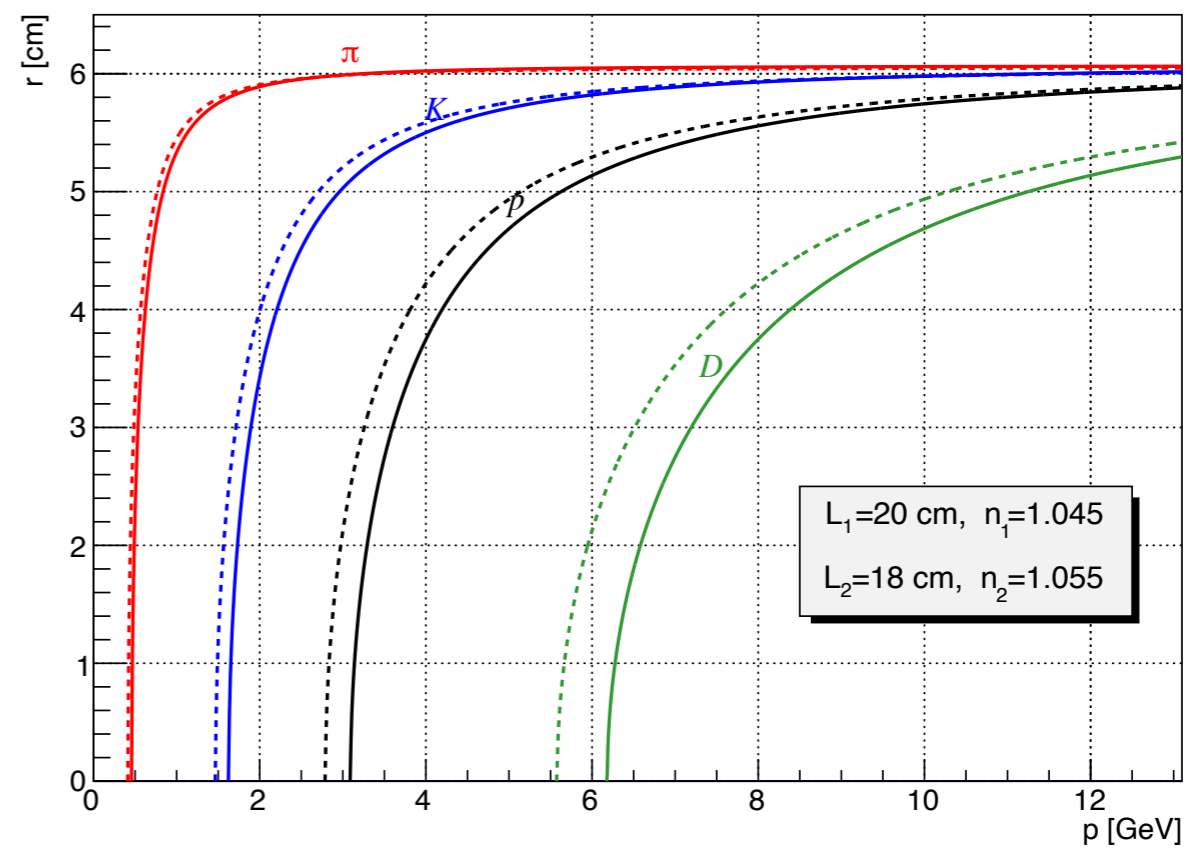
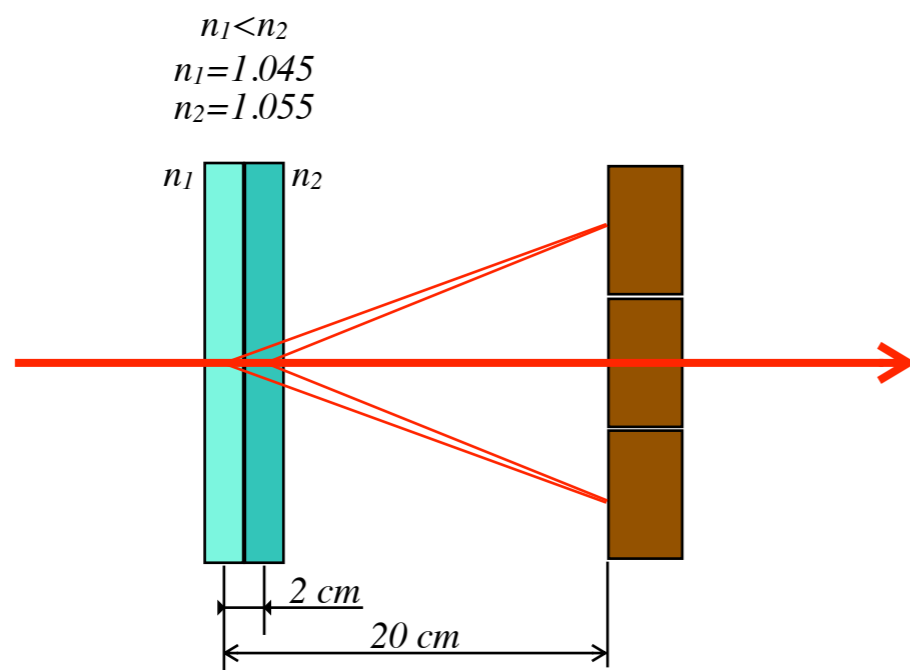
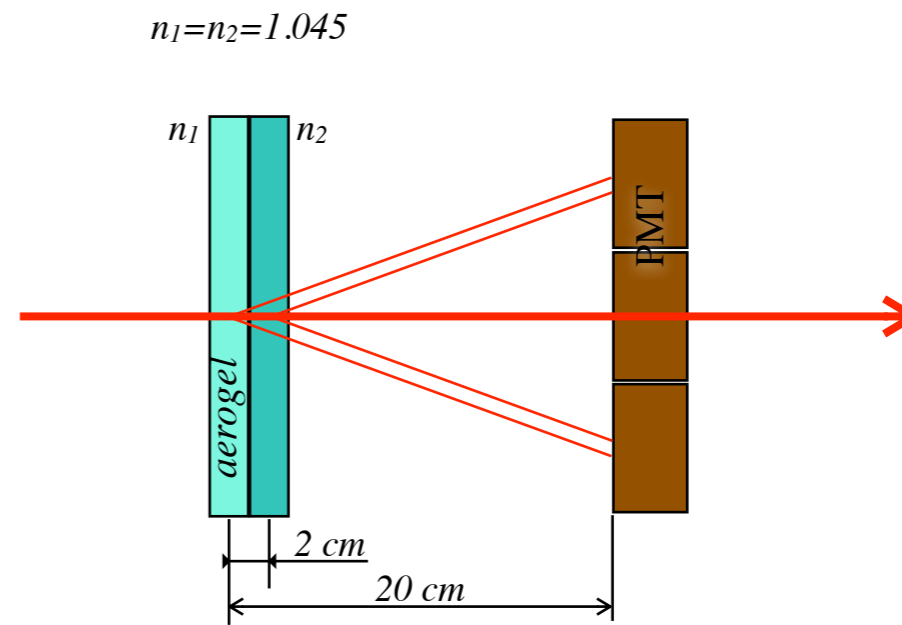
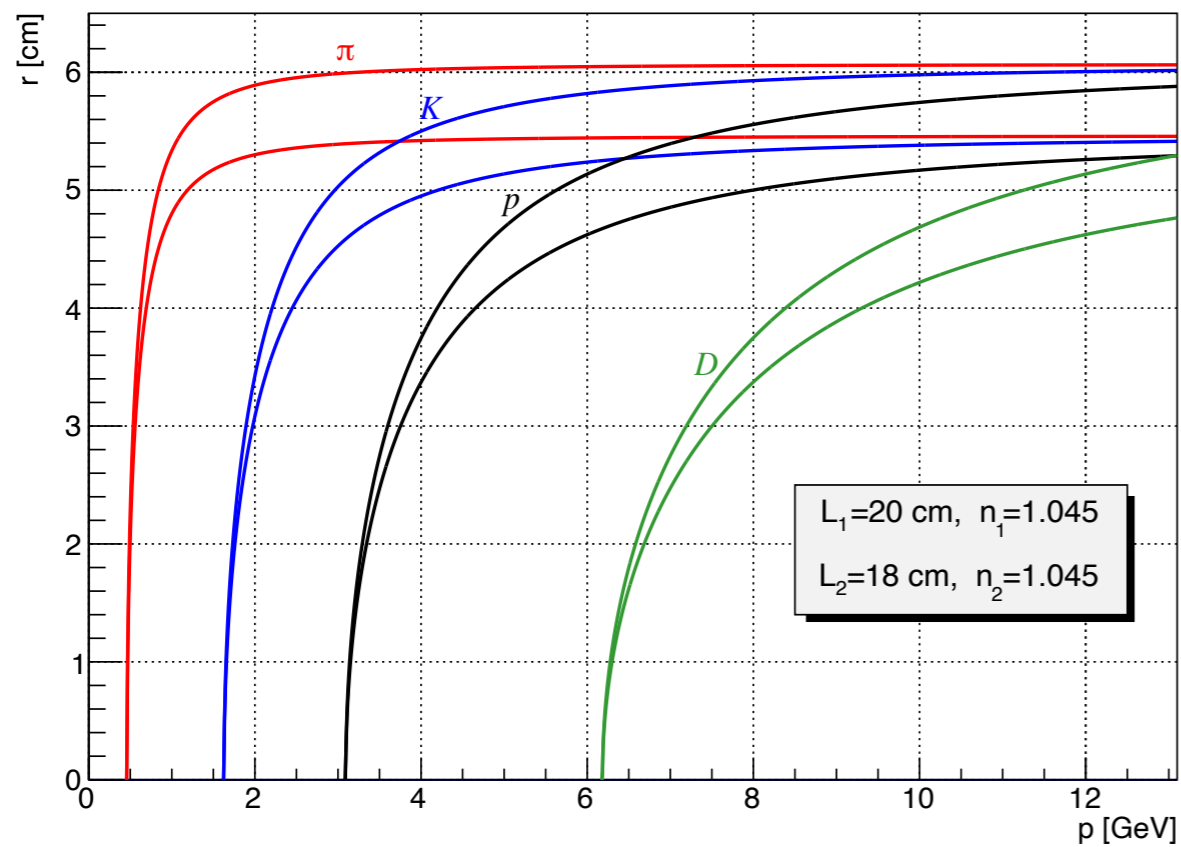
- Focusing effect using  $n_1=1.045$  and  $n_2=1.055$
- Mass production in 2014
- Ref: *NIMA 876 (2017) 129*



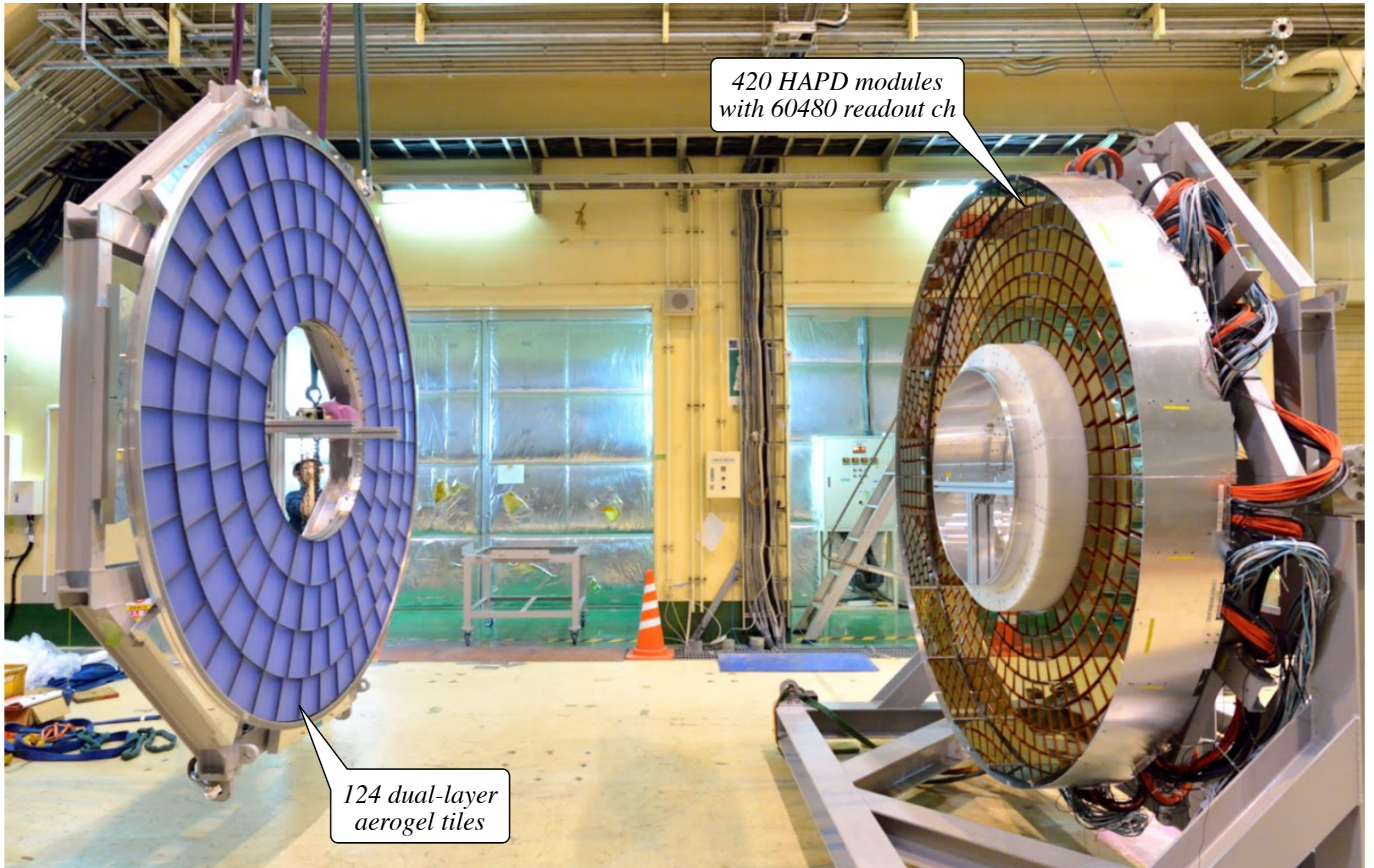
## HAPD (Hybrid Avalanche Photo Detector)



- $R_\pi - R_K = 5 \text{ mm}$  for  $p = 4 \text{ GeV} \rightarrow$  pixel size is 5 mm
- Ref: *PTEP 2016 (2016) 3, 033H01 [1603.02503]*



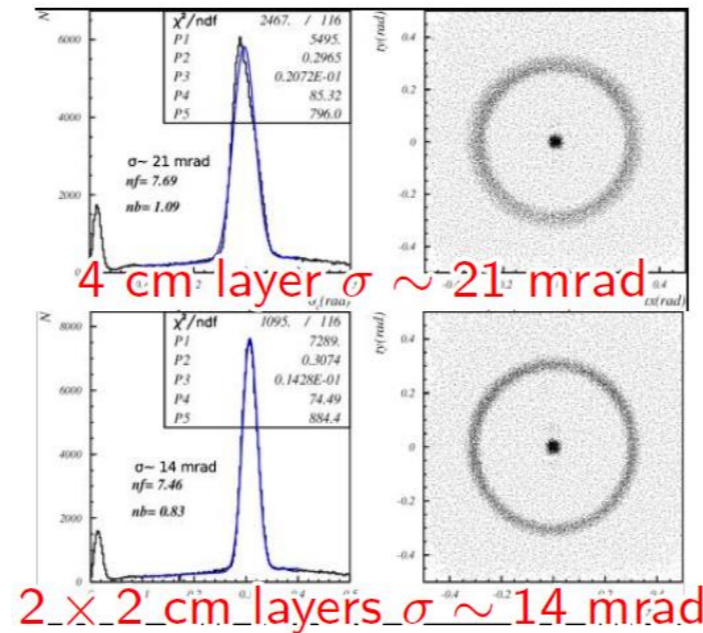
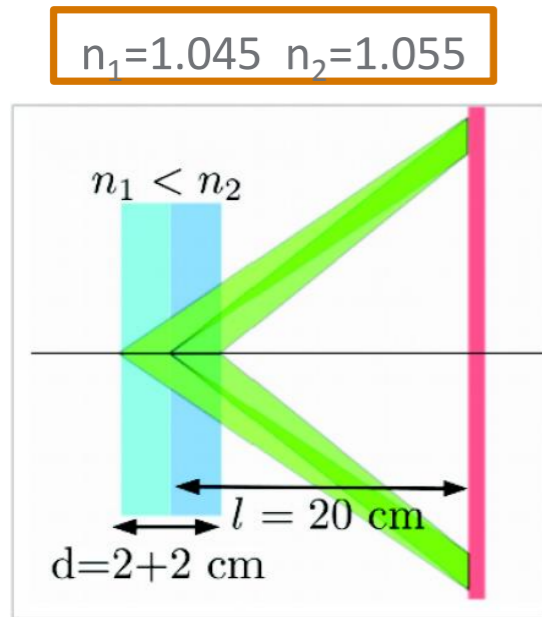
# ARICH (in endcap) of the Belle II experiment



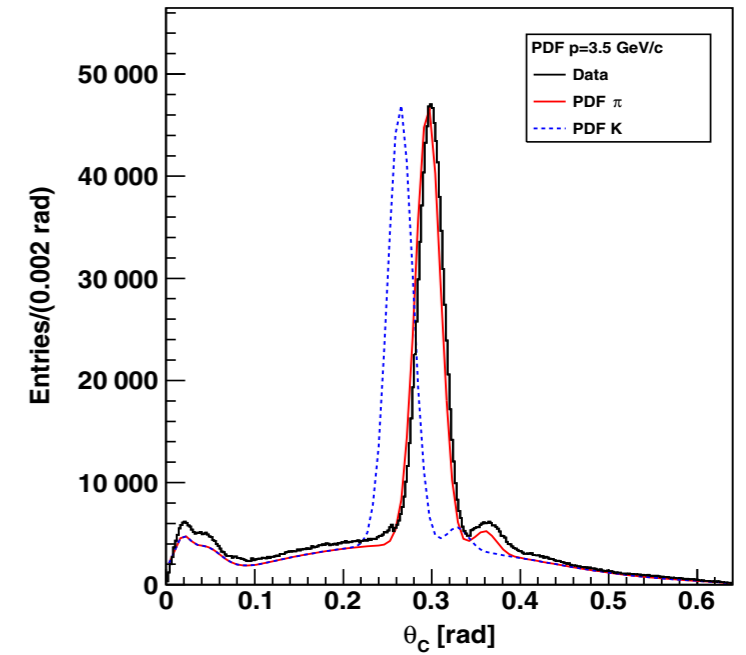
*Installed in Oct 2017*

# ARICH (in endcap) of the Belle II experiment

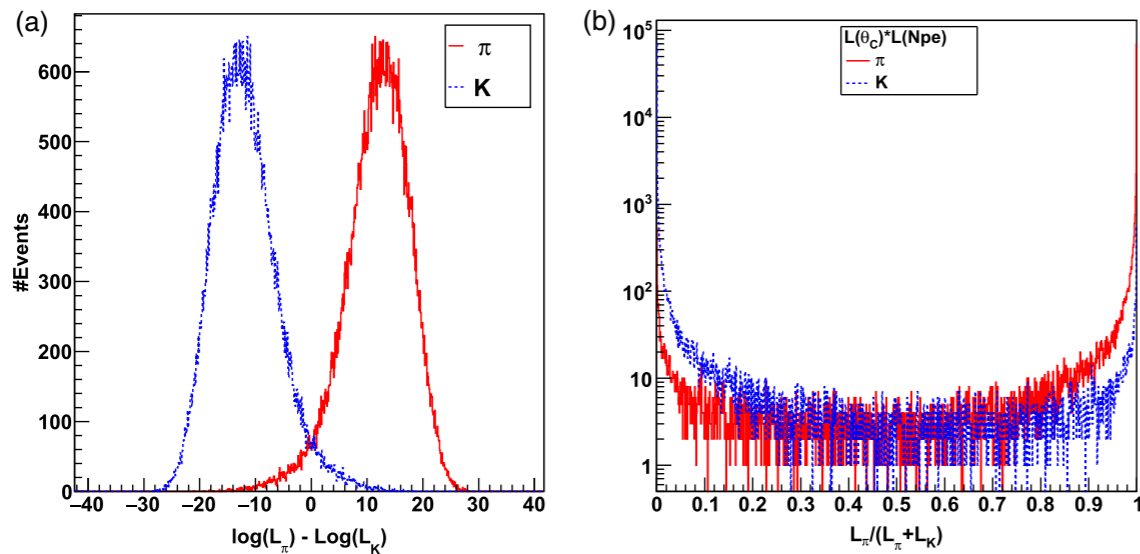
## Focusing principle



## Cherenkov angle for $\pi$ and K



## $\pi$ and K likelihoods



The difference between the likelihoods

Likelihood ratio distribution

**Fig. 15.** (a) Distribution of the likelihood difference between the pion (solid line) and kaon (dashed line) at 3.5 GeV/c. (b) Likelihood ratio distribution for pions and kaons at 3.5 GeV/c.

## Efficiency of $\pi$ and K identification

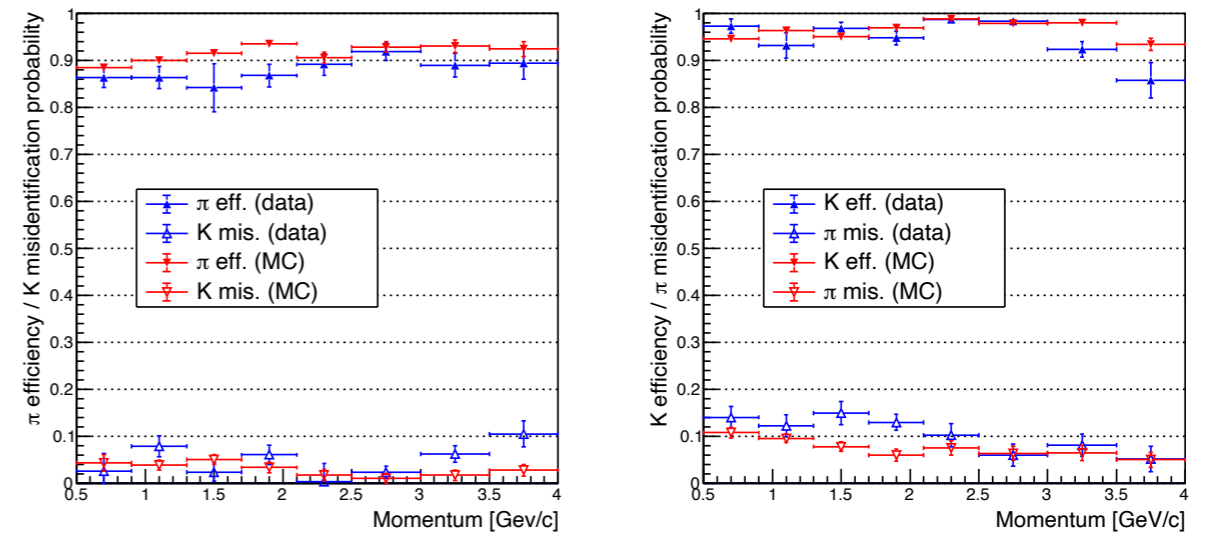
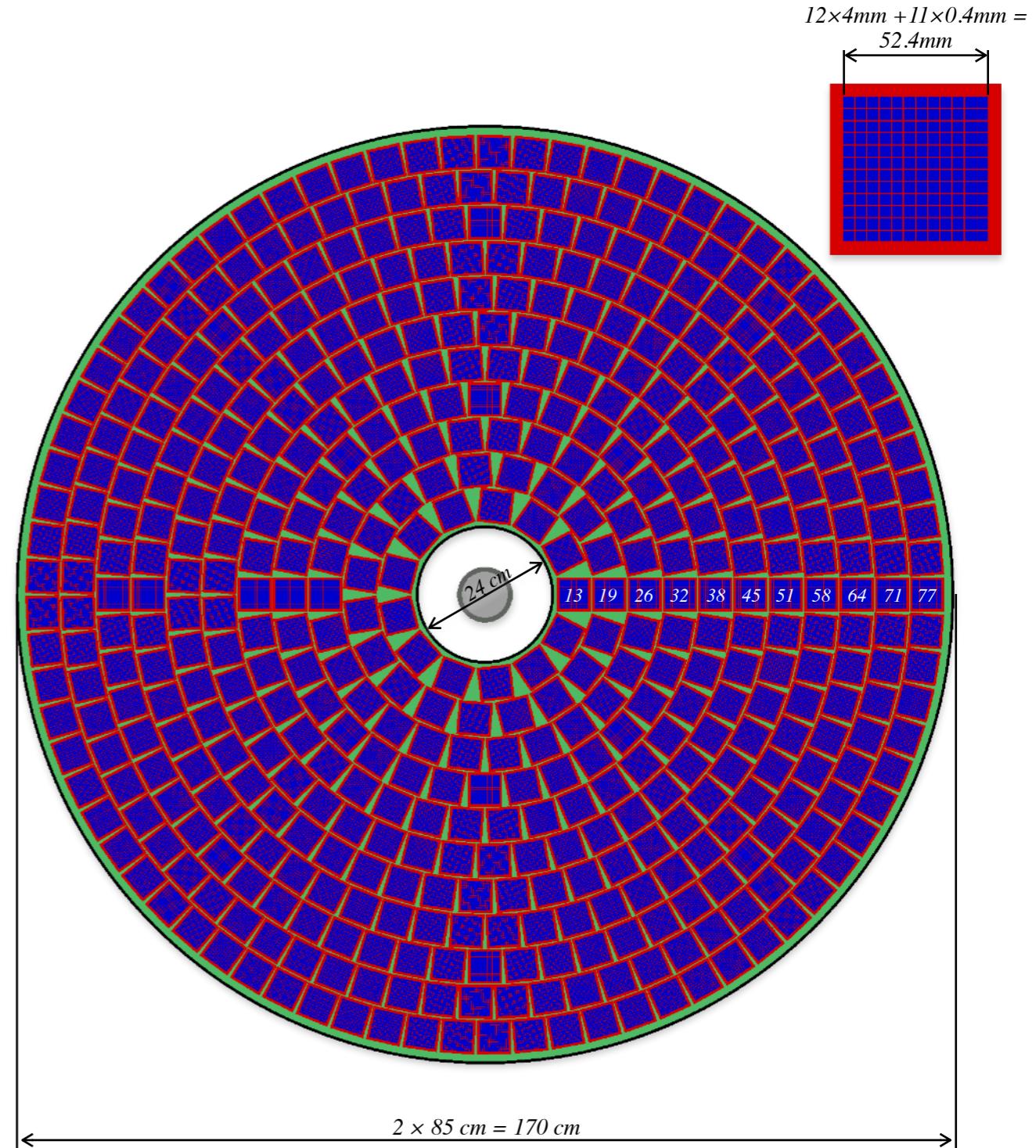
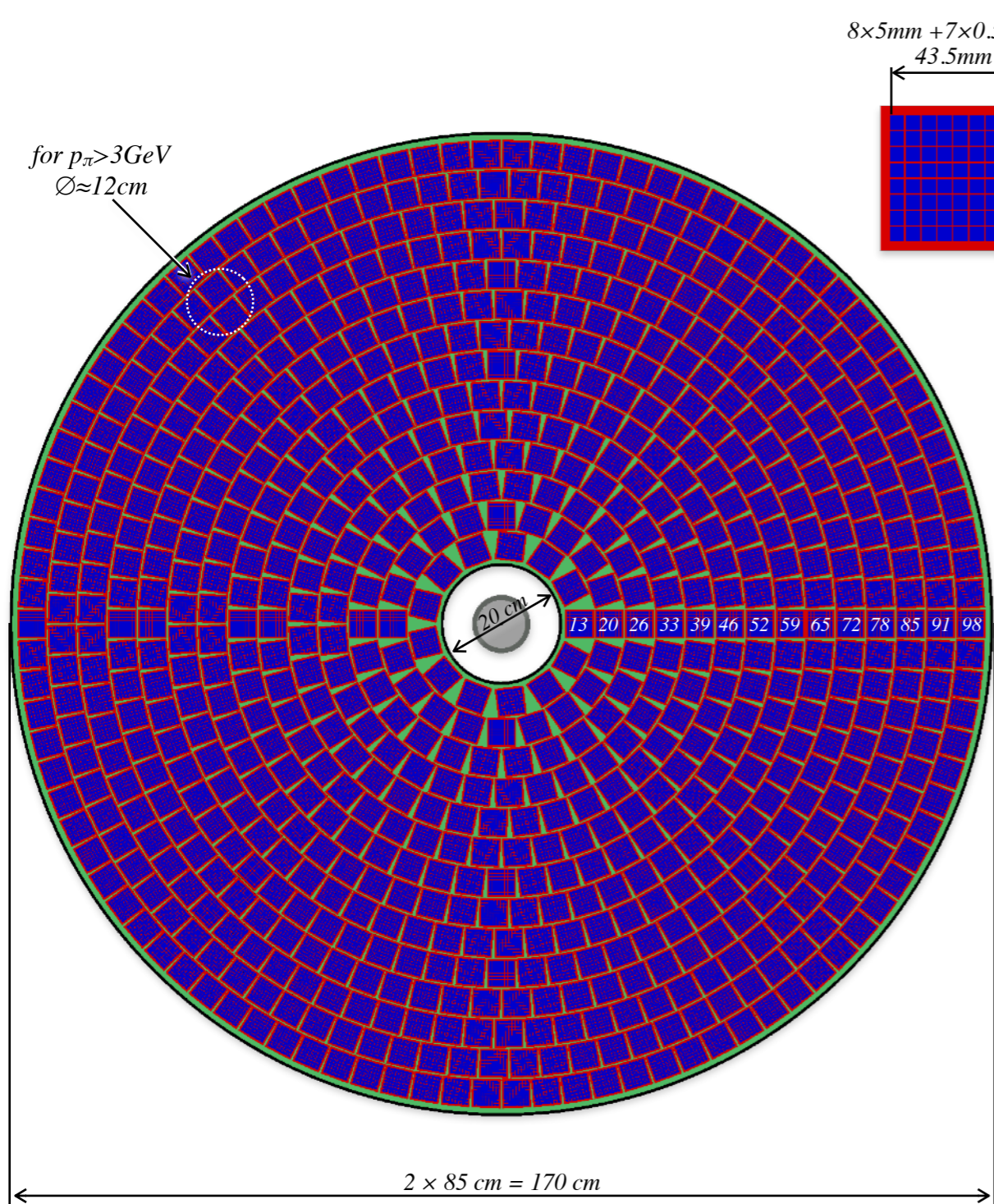


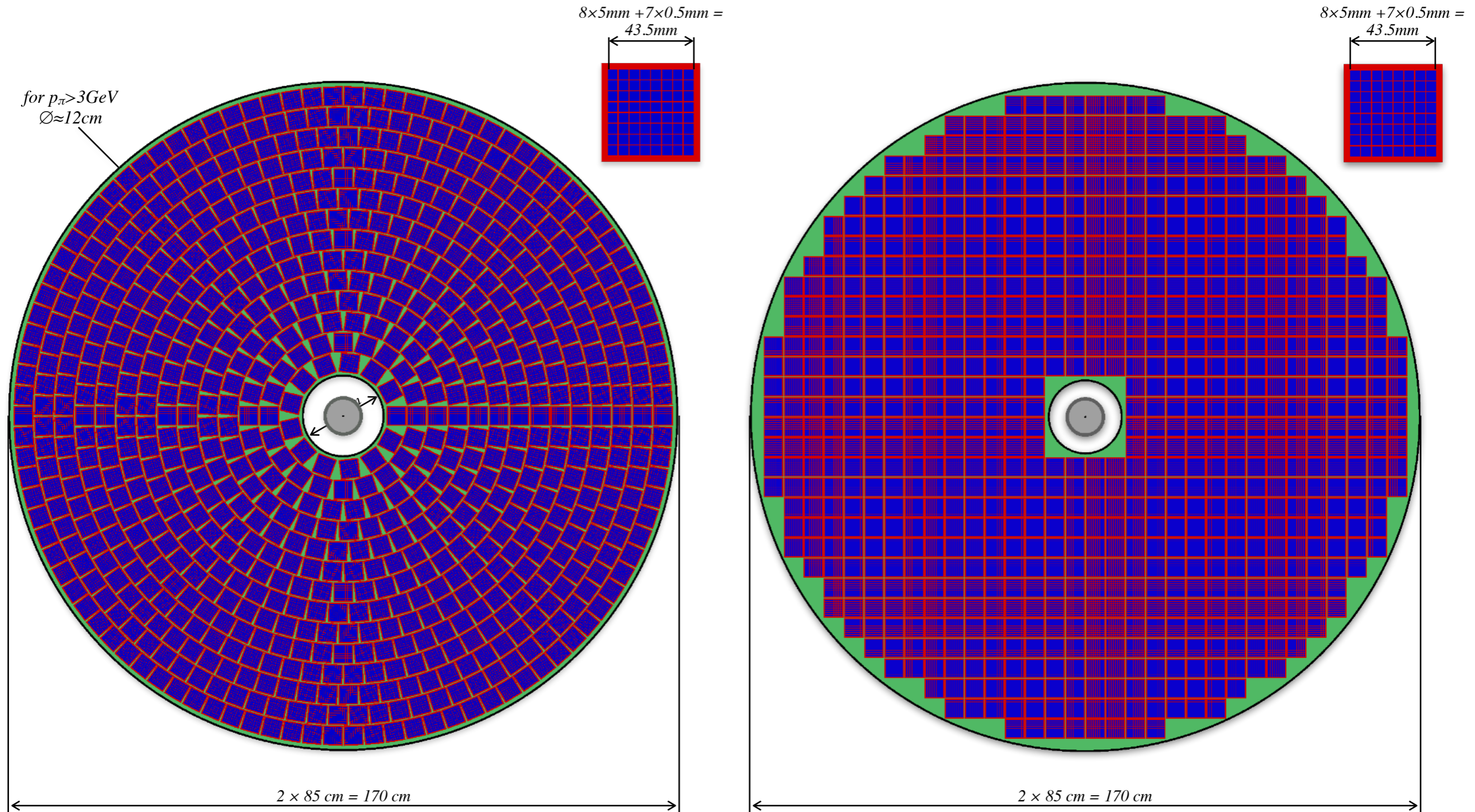
**Figure 14:** Efficiency and misidentification probability as a function of the momentum:  $\pi$  efficiency and  $K$  misidentification probability (left), and  $K$  efficiency and  $\pi$  misidentification probability (right).

Multi-Anode MCP-PMT:  $8 \times 8 = 64$  pads,  $S_{\text{pad}} = 5 \times 5 \text{ mm}^2$   
 $S_{\text{ARICH}} = 2.2 \text{ m}^2$ ,  $N_{\text{PMT}} = 777$ , filling=56%,  $N_{\text{ch}} = 777 \times 64 \approx 50\text{k}$

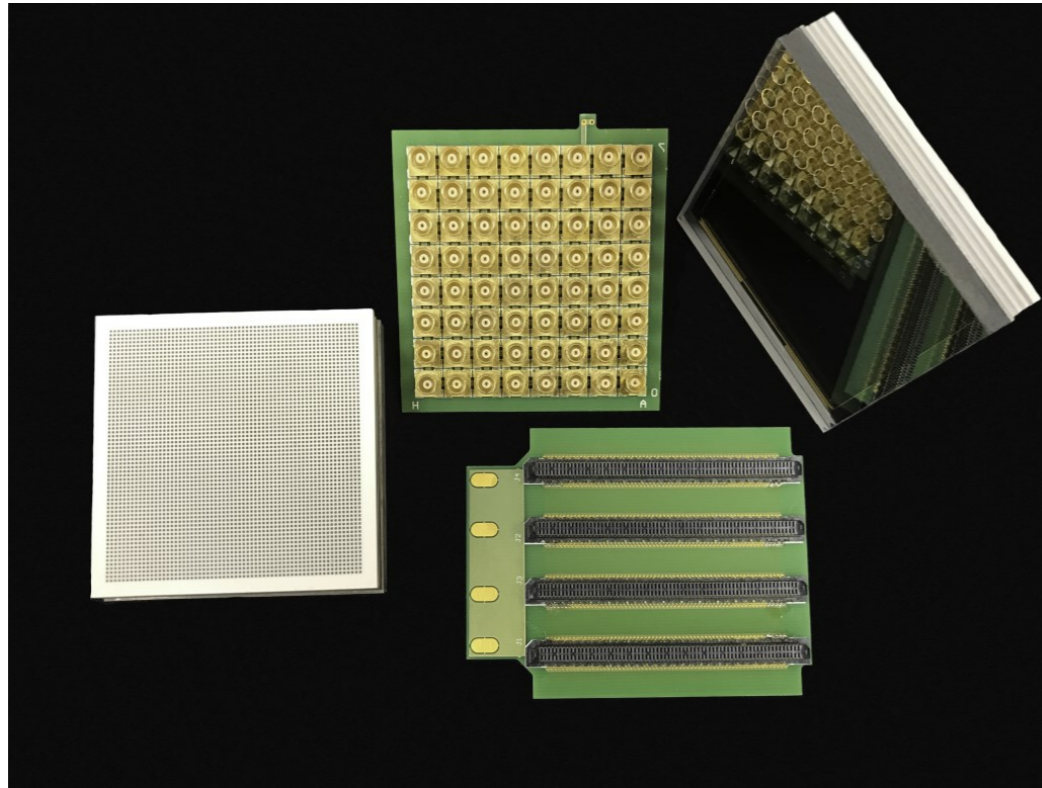
Multi-Anode MCP-PMT:  $12 \times 12 = 144$  pads,  $S_{\text{pad}} = 4 \times 4 \text{ mm}^2$ ,  
 $S_{\text{ARICH}} = 2.2 \text{ m}^2$ ,  $N_{\text{PMT}} = 494$ , filling=51%,  $N_{\text{ch}} = 494 \times 144 \approx 71\text{k}$



# Different PMT layouts







## APPLICATIONS

- ◆ Ring Imaging Cherenkov (RICH)
- ◆ Detection of Internally Reflected Cherenkov (DIRC)
- ◆ Sampling Calorimeter Readout
- ◆ Wavelength Shifting Fibre Readout
- ◆ Scintillating/Cherenkov Fibre Readout
- ◆ Beam Monitor
- ◆ High Content Screening
- ◆ Time Resolved Spectroscopy
- ◆ LIDAR
- ◆ Standoff Chemical/Biological Detection
- ◆ Microplate Readout

## PRODUCT OVERVIEW

### General Characteristics

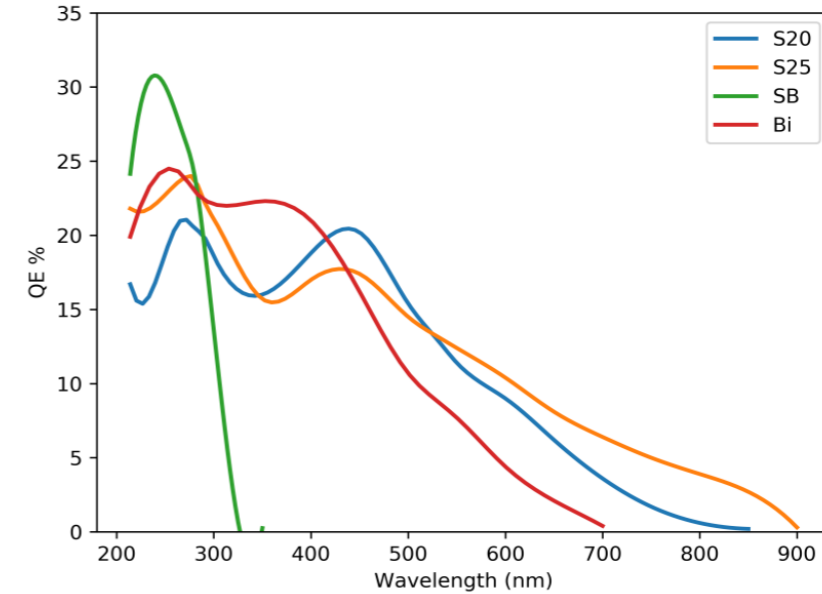
Window	Fused Silica (Optional Fibre Optic)
Active Area	53 x 53 mm
Electron Multiplier	Dual MCP
Anode Format	64 x 64 (Reconfigurable)
Anode Pitch	0.828 mm
Photocathode	Solar Blind, Bi-Alkali, S20, S25

## SPECIFICATIONS

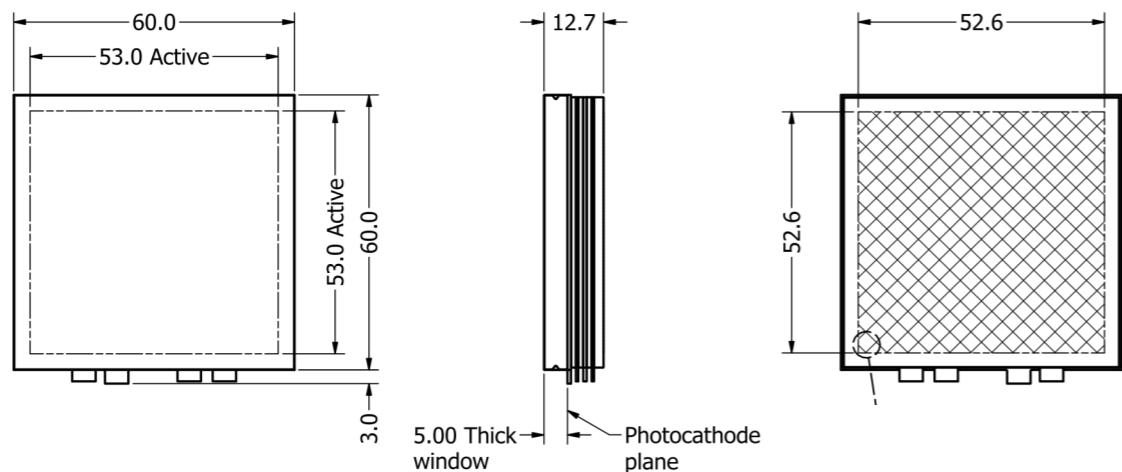
Single Photon Response	Typical
Dark Counts per Anode	< 2 cps
Pulse Risetime (10% to 90%)	<175 ps
Pulse Width	<430 ps FWHM
Transit Time Spread	<40 ps RMS
Pulse Height Distribution	100% FWHM
Linear Total Count Rate	Up to 10 MHz

Maximum Ratings	
Overall Voltage	< 3500 V
Operating Temperature	-50 to +50°C
Storage Temperature	-50 to +50°C

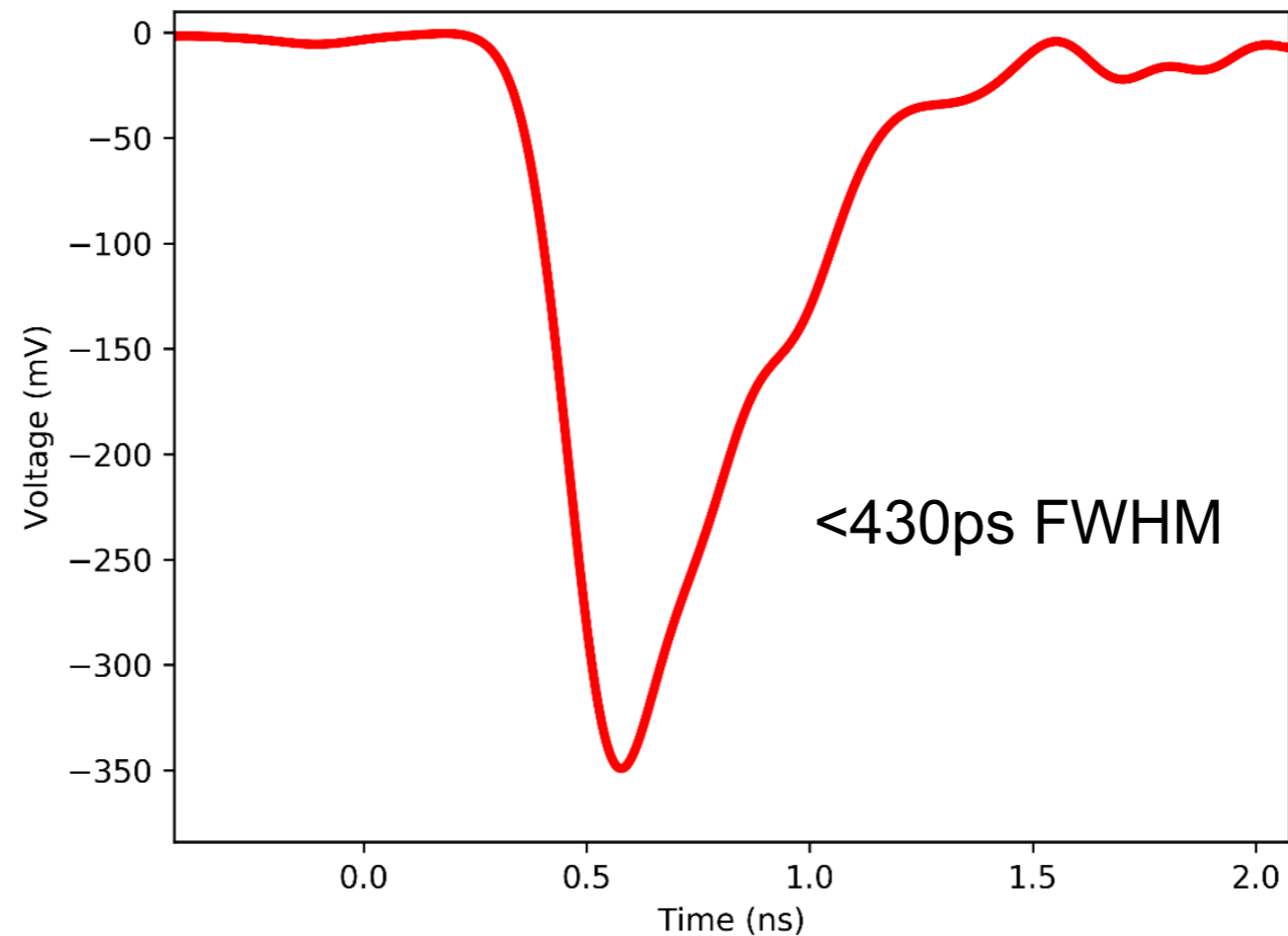


Available photocathodes on fused silica window. Optional fibre optic window will reduce sensitivity and no response below 300 nm.



Anode Format	Pitch		Total Anodes
	X (mm)	Y (mm)	
32 x 32	0.88	0.88	1024
16 x 16	1.76	1.76	256
32 x 8	0.88	0.88	256
8 x 8	3.52	3.52	64

## Single anode signal



Average of 50 single photon pulses measured on 5 GHz, 20 GS/s scope, using a Photek LPG-405 pulsed laser.

backup slides

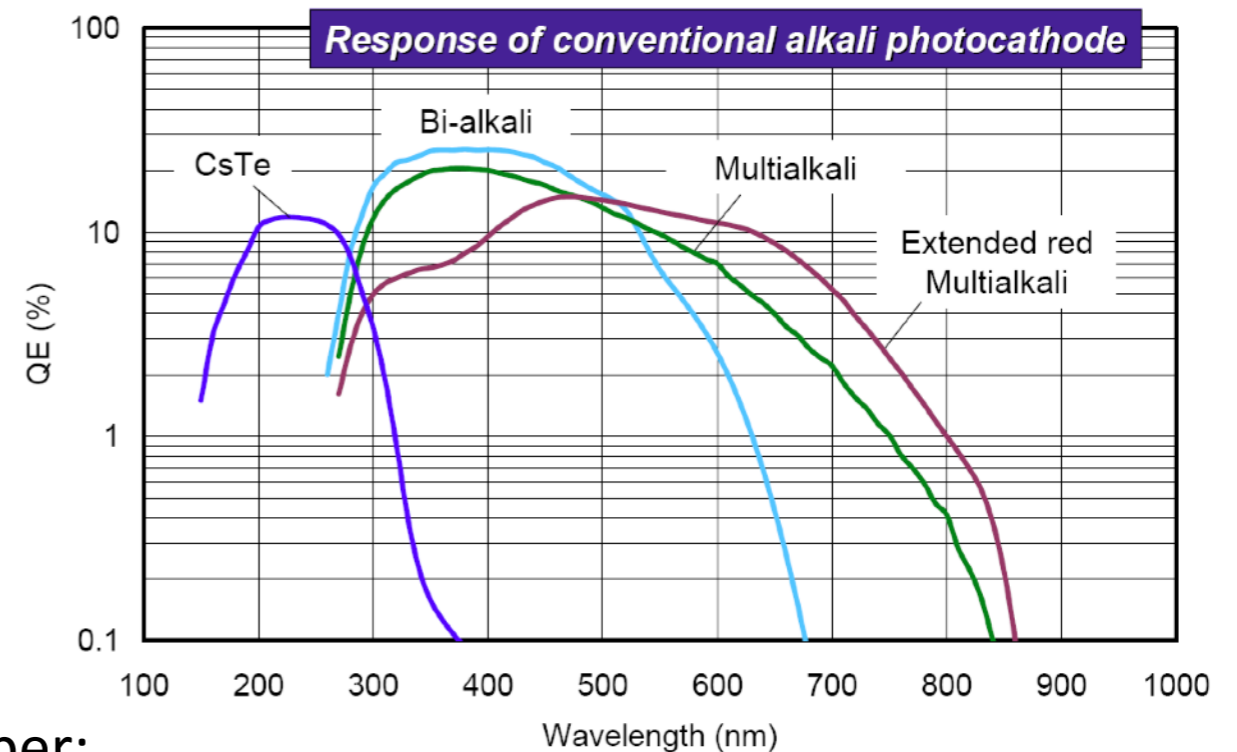
## What signal can we have in SPD with the PMT as a photon detector?


The most suitable type of the photocathodes for detection of the Cherenkov light is Bi-alkali (Sb-K-Cs, Rb-Sb-Cs), with sensitivity extending from ~260 to 650 nm and maximum QE~20% between 300 and 500 nm.

$$N = 2\pi\alpha l \left( \frac{1}{\lambda_1} - \frac{1}{\lambda_2} \right) \sin^2\theta$$

Parameters used in calculation of the p.e. number:

- aerogel thickness                      20 mm,  $n=1.045$  + 20 mm,  $n=1.055$
- effective area of the MCP              60%
- sensitive area of the detector        60%
- quantum efficiency                      20% at 300-500 nm  
    10% at 270-300 and 500-550 nm



The number of photoelectrons calculated without account of the light losses 

	$\pi$	K	p
1 GeV/c	44	---	---
2	52	21	---
3	54	41	1
4	54	46	26
5	54	49	36

Transmission length at  $\lambda=400$  nm (from BELLE-II):

47 mm at  $n= 1.0451$

36 mm at  $n= 1.0547$

Then, in our case (20mm  $n=1.045$  + 20mm  $n=1.055$ ) transmission will be (roughly)  $\approx 60\%$

and the number of photoelectrons, i.e. points on the Cherenkov ring 

	$\pi$	K	p
1 GeV/c	26	---	---
2	31	13	---
3	32	25	---
4	32	28	16
5	32	29	22

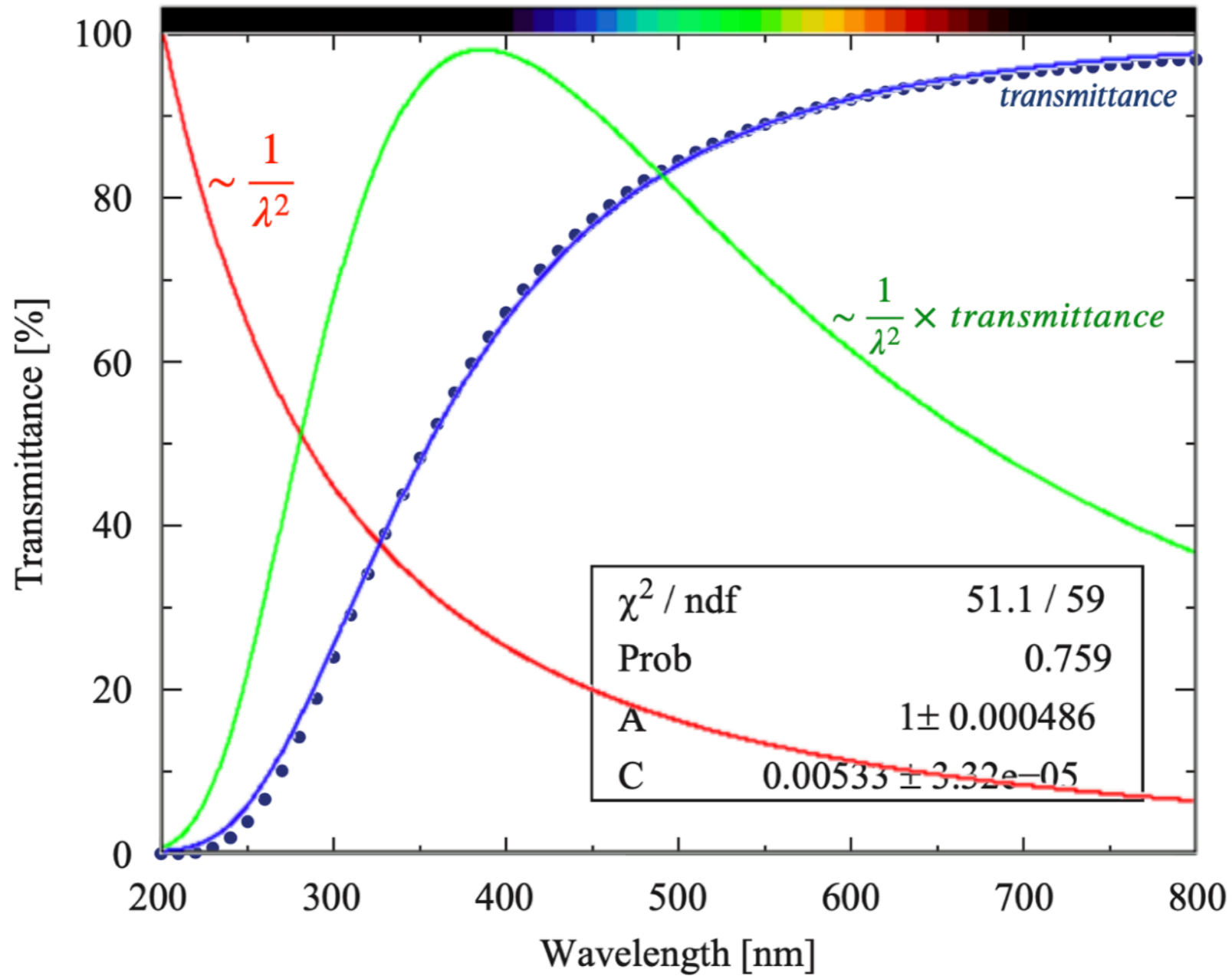
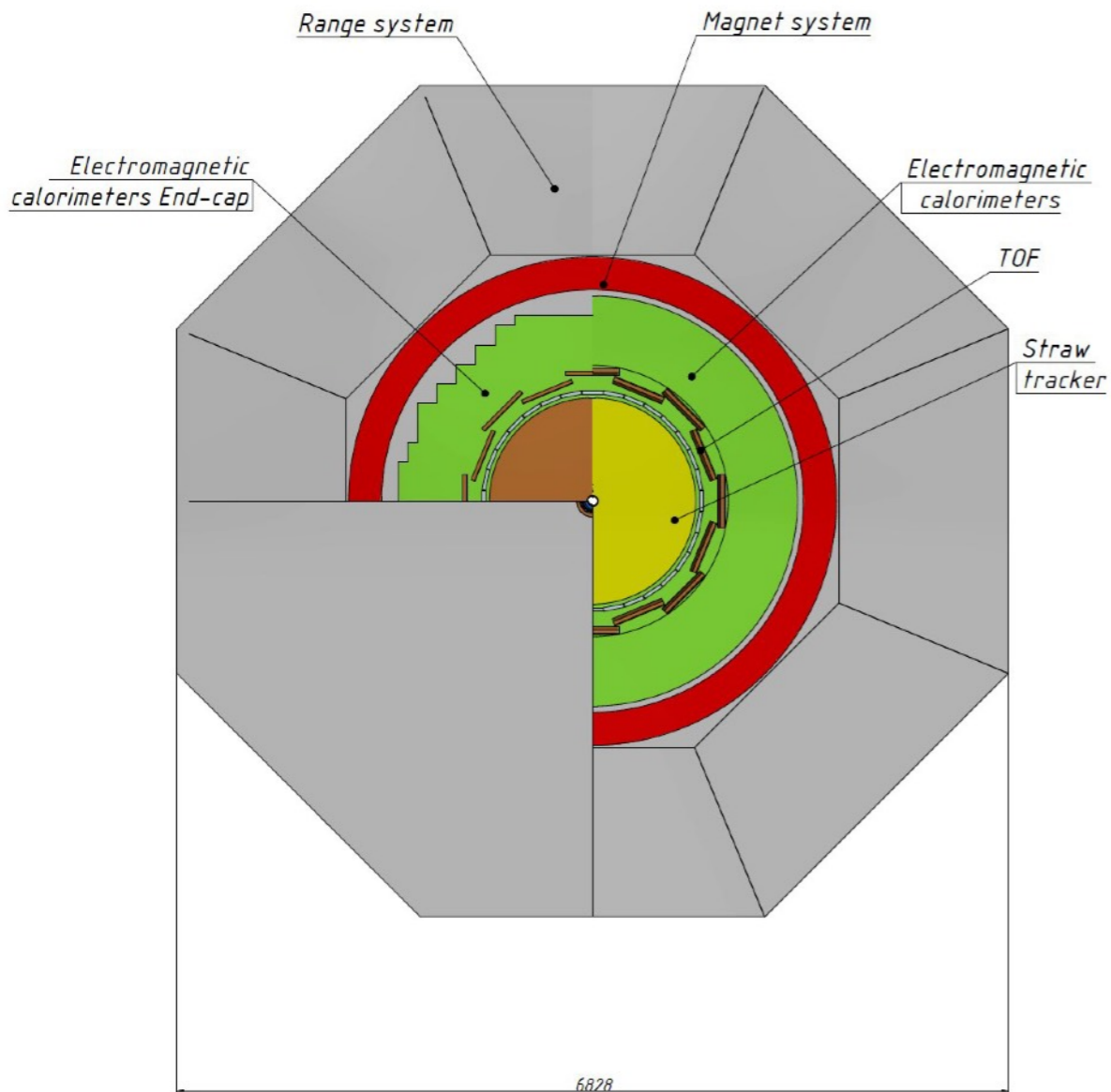
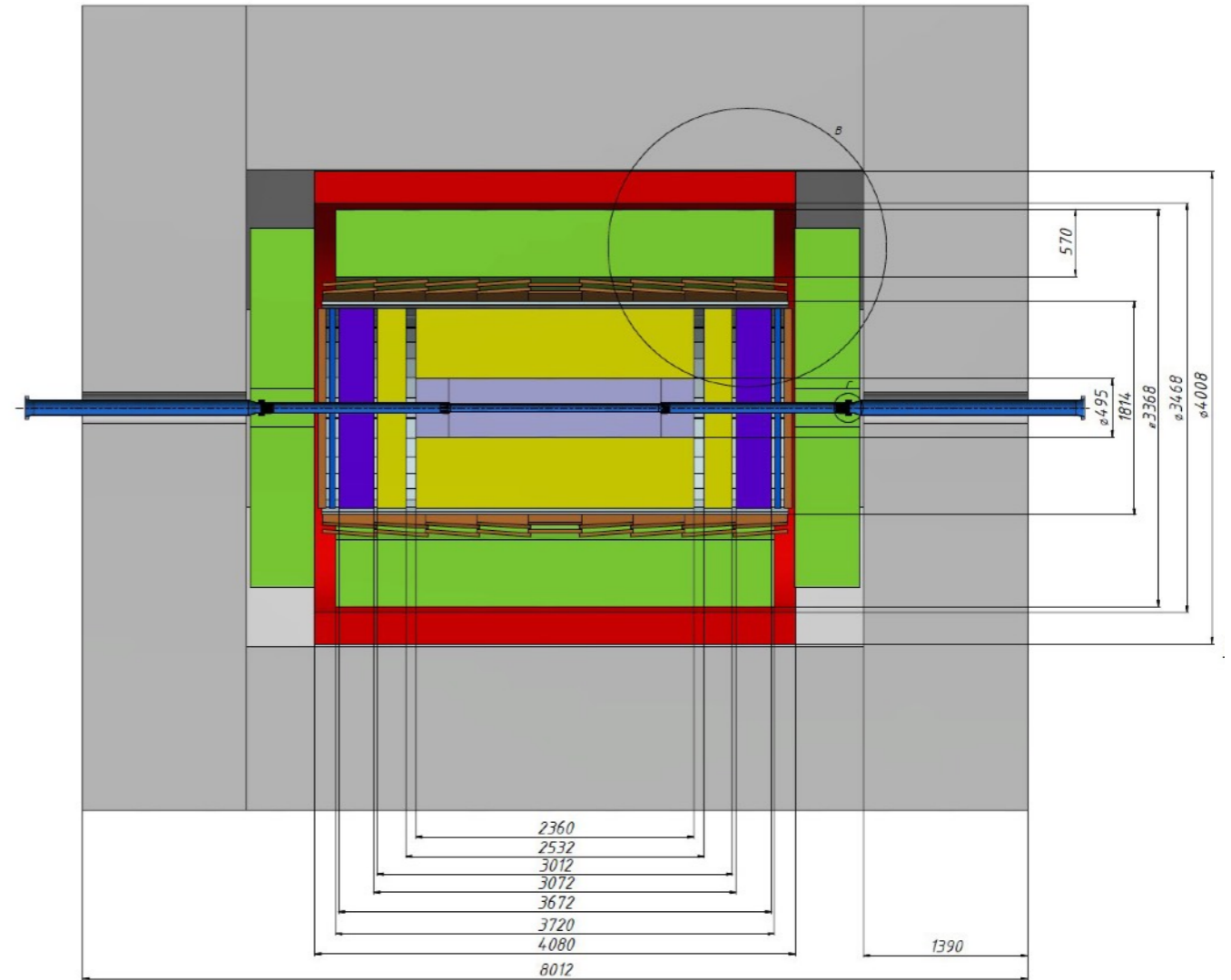


**Fig. 6.** Aerogel transmittance curve for aerogel ID=PDR21-2a,  $n=1.044$ , and  $t=20.8$  mm. Circles show the transmittance measured every 10 nm by the spectrophotometer and the solid line shows the fit. The parameters obtained from the fitting with  $T=A \exp(-Ct/\lambda^4)$  are  $A=1$  and  $C=0.00533 \pm 0.00003 \mu\text{m}^4/\text{cm}$ . The upper limit of the parameter  $A$  was set to 1 in the fitting procedure. The corresponding transmission length was calculated to be 50 mm at  $\lambda = 400$  nm.

# SPD setup (Mar 2023)



A





# SPD setup (Mar 2023)

